

Form factors of vector and axial-vector mesons in holographic D4-D8 model

C. A. Ballon Bayona[†], Henrique Boschi-Filho^{‡,a}, Nelson R. F. Braga^{‡,b} and Marcus A. C. Torres^{‡,c}

[†]*Centro Brasileiro de Pesquisas Físicas, Rua Dr. Xavier Sigaud 150, Urca, 22290-180, Rio de Janeiro, RJ, Brazil*
e-mail: ballon@cbpf.br

[‡]*Instituto de Física, Universidade Federal do Rio de Janeiro, Caixa Postal 68528, RJ 21941-972, Brazil*
^ae-mail: boschi@if.ufrj.br; ^be-mail: braga@if.ufrj.br; ^ce-mail: mtorres@if.ufrj.br

ABSTRACT: We calculate elastic and non-elastic electromagnetic form factors for vector and axial-vector mesons in the holographic D4-D8 brane model. We obtain the mass spectrum and Regge trajectories for these particles. From the elastic form factors we extract the electric radius, the magnetic and quadrupole moments. Form factors for transverse and longitudinal polarizations are also obtained. We find superconvergence sum rules for the vector and axial-vector meson couplings that determine the asymptotic behavior of the form factors at large momentum transfer. Our results show good agreement with other holographic models and QCD.

KEYWORDS: Gauge-gravity correspondence, AdS-CFT Correspondence.

Contents

1. Introduction	1
2. D4-D8 Model	2
2.1 The D4 background	3
2.2 The D8-brane solution	3
3. Vector and axial-vector mesons	4
3.1 Wave functions and Regge trajectories	6
3.2 Coupling and decay constants	8
4. Form Factors	9
4.1 Elastic case	11
4.2 Non-elastic case	15
5. Conclusion	16

1. Introduction

Recently a holographic model for large N_c QCD with massless quarks at strong coupling was proposed [1,2] (see also [3–5]). This model consists on the intersection of N_c D4-branes and N_f D8- $\overline{\text{D8}}$ pairs of branes in type IIA string theory in the limit $N_f \ll N_c$. The numbers N_c and N_f are interpreted as the color and flavor numbers of strongly coupled QCD like theory. A remarkable feature of the D4-D8 brane model is the holographic description of chiral symmetry breaking $U(N_f)_L \times U(N_f)_R \rightarrow U(N_f)$ from the merging of the D8- $\overline{\text{D8}}$ branes.

One important property of the D4-D8 brane model is the explicit realization of vector meson dominance [6, 7] which states that the interaction of a hadron with a photon is mediated by vector mesons. Therefore, the calculation of hadronic form factors involve a sum over all intermediate vector mesons that, in this model, correspond to the Kaluza Klein modes of an extra compact dimension. This property makes the D4-D8 model an important tool to describe the electromagnetic interaction of hadrons. In particular, the results for the pion form factor obtained in ref. [2] present good agreement with available experimental data.

In this article we use the D4-D8 brane model to study the electromagnetic interactions of vector and axial-vector mesons. First we obtain numerically the wave functions that arise in the Kaluza Klein expansion in the compact extra dimension. The associated eigenvalues give us the meson mass spectra and Regge trajectories. We calculate the relevant decay

constants and the couplings of three-meson vertices. Using these results we obtain the electromagnetic elastic and transition form factors for vector and axial-vector mesons.

We analyse the momentum dependence of these form factors in the limit of large space-like momentum transfer. We find superconvergence sum rules for the vector and axial-vector meson coupling constants that determine the asymptotic behavior of the form factors. These sum rules generalize a previous result for the ρ meson obtained within the hard wall model [8].

From the elastic form factors, we extract the electric radius, the magnetic and quadrupole moments for the ρ and a_1 mesons. We calculate the elastic form factors F_{TT} , F_{LT} , F_{LL} that arise from the decomposition of the initial and final meson polarizations into transversal and longitudinal components. We find that the asymptotic behavior of these form factors in the D4-D8 model is in agreement with QCD predictions.

Electromagnetic form factors of vector mesons in other holographic models have been studied in [8–12]. For a review of mesons in holographic models see [13]. Form factors of baryons have been calculated recently in the D4-D8 brane model by considering instanton configurations [4, 5].

2. D4-D8 Model

The Sakai-Sugimoto D4-D8 model is built adding N_f pairs of D8 and $\overline{\text{D8}}$ probe branes in the spacetime background formed by the presence of N_c D4 branes. Initially, the branes are set in the following spacetime configuration:

	0	1	2	3	(4)	5	6	7	8	9
D4	○	○	○	○	○					
D8 - $\overline{\text{D8}}$	○	○	○	○		○	○	○	○	○

The brane worldvolumes are extended in the directions indicated by ○. The four directions x_0, \dots, x_3 correspond to our four-dimensional Minkowski space-time and the direction x_4 is compactified in a circle.

The low energy spectrum of open strings in the D4-D8 geometry includes gauge fields in the adjoint representation (arising from 4-4 strings) and quarks in the fundamental representation (coming from 4-8 strings) of the group $U(N_c)$. All these fields live in a 5d space-time with a compact coordinate where fermionic anti-periodic conditions are imposed in order to break supersymmetry.

Since the quarks D4-D8 and D4- $\overline{\text{D8}}$ have different chirality we would expect the presence of chiral symmetry $U(N_f)_L \times U(N_f)_R$. However the background forces the branes D8 and $\overline{\text{D8}}$ to be united in a single stack of N_f D8 branes, breaking chiral symmetry $U(N_f)_L \times U(N_f)_R$ into a remaining $U(N_f)$.

2.1 The D4 background

The D4-brane solution consists on the space-time metric

$$ds^2 = \left(\frac{U}{R}\right)^{3/2} [\eta_{\mu\nu} dx^\mu dx^\nu + f(U) d\tau^2] + \left(\frac{R}{U}\right)^{3/2} \left[\frac{dU^2}{f(U)} + U^2 d\Omega_4^2 \right], \quad (2.1)$$

with $f(U) = 1 - (U_{KK}/U)^3$, and the dilaton and RR form

$$e^\Phi = g_s \left(\frac{U}{R}\right)^{3/4}, \quad F_4 = \frac{3N_c}{4\pi} \epsilon_4. \quad (2.2)$$

The x^μ represent the 4d coordinates in Minkowski spacetime with metric $\eta_{\mu\nu}$, while τ is the compactified x_4 direction, with period $\delta\tau$. The x_5, \dots, x_9 are written in spherical coordinates, with U its radial direction. The constant R is related to the string length $\sqrt{\alpha'}$ and string coupling g_s by $R^3 = \pi g_s N_c \alpha'^{3/2}$ while ϵ_4 is the volume form.

The radial coordinate has a minimum U_{KK} related to the period of the τ coordinate by

$$\delta\tau = \frac{4\pi R^{3/2}}{3 U_{KK}^{1/2}}, \quad (2.3)$$

which is obtained from the singularity avoidance condition. The Kaluza-Klein modes associated with the compact τ coordinate will thus have a natural mass scale

$$M_{KK} \equiv \frac{2\pi}{\delta\tau} = \frac{3 U_{KK}^{1/2}}{2 R^{3/2}}. \quad (2.4)$$

The effective four dimensional Yang-Mills coupling is related to the string coupling by

$$g_{YM}^2 = 2\pi \sqrt{\alpha'} M_{KK} g_s. \quad (2.5)$$

2.2 The D8-brane solution

The D8-brane is localized by imposing a relation between the radial coordinate U and the compact coordinate τ in (2.1). The configuration $U = U(\tau)$ has to minimize the Dirac-Born-Infeld action

$$\begin{aligned} S_{D8} &= -\mu_8 \int d^4x d\tau d^4\Omega e^{-\Phi} \sqrt{-\det \mathcal{P}[G]_{AB}} \\ &\sim \int d\tau U^4 \sqrt{f(U) + \frac{R^3 U'^2}{U^3 f(U)}} \end{aligned} \quad (2.6)$$

where $\mu_8 = (2\pi)^{-8} \alpha'^{-9/2}$ is the D8 brane tension, $\mathcal{P}[G]_{AB}$ is the induced metric of the D8 brane, and $U' = dU/d\tau$. We are looking for a brane configuration symmetric in τ with a minimum value U^* . Then, the appropriate boundary conditions are $U'(0) = 0$ and $U(0) = U^*$. Since the action does not depend explicitly on τ we can easily find $U(\tau)$ as a solution to the energy conservation equation

$$\left(\frac{U^4 f(U)}{\sqrt{f(U) + \frac{R^3 U'^2}{U^3 f(U)}}} \right) = U_*^4 \sqrt{f(U_*)}, \quad (2.7)$$

After imposing the Sakai-Sugimoto condition $U_* = U_{KK}$ the D8-brane equation reduces to

$$\frac{d\tau}{dU} = \begin{cases} 0 & \text{for } U > U_{KK} \\ \pm\infty & \text{for } U = U_{KK} \end{cases}, \quad (2.8)$$

which has a box-type solution consisting on two parallel lines $\tau(u) = \pm\delta\tau/4$ plus a perpendicular line $U = U_{KK}$. In the dual gauge theory, the condition $U_* = U_{KK}$ can be interpreted as a zero mass condition for the quarks. It is convenient to define the coordinates

$$r = U_{KK} \sqrt{\frac{U^3}{U_{KK}^3} - 1}, \quad \theta = \frac{2\pi}{\delta\tau} \tau, \quad (y, z) = (r \cos \theta, r \sin \theta), \quad (2.9)$$

so that the D8-brane solution is simply $y = 0$ with the z coordinate running from $-\infty$ to ∞ . The D8-brane metric then can be written as [1]

$$ds_{D8}^2 = \left(\frac{U_z}{R}\right)^{3/2} \eta_{\mu\nu} dx^\mu dx^\nu + \frac{4}{9} \left(\frac{R}{U_z}\right)^{3/2} \frac{U_{KK}}{U_z} dz^2 + R^{3/2} U_z^{1/2} d\Omega_4^2, \quad (2.10)$$

with

$$U_z = U_{KK} \left(1 + \frac{z^2}{U_{KK}^2}\right)^{1/3}. \quad (2.11)$$

Finally, the probe limit condition $N_f \ll N_c$ assures that the D4 background deformation by the D8/ $\overline{D8}$ branes can be neglected. This condition can be interpreted in the dual theory as a quenching limit, where the quark loops are singled out.

3. Vector and axial-vector mesons

In the D4-D8 model, mesons of the dual gauge theory emerge as states of open strings connecting the D8- $\overline{D8}$ branes. These states correspond to fluctuations of the D8 branes solutions in the D4 background. In particular, vector and axial-vector mesons are described by $U(N_f)$ gauge field fluctuations. The dynamics of these fluctuations is given by the action

$$S_{D8} = (\pi\alpha')^2 \mu_8 \int d^4x dz d^4\Omega e^{-\Phi} \sqrt{-\det g} \text{tr}(F^{MN} F_{MN}) + S_{CS}, \quad (3.1)$$

where $F_{MN} = \partial_M A_N - \partial_N A_M + [A_M, A_N]$ is the field strength with $A_M = (A_\mu, A_z, A_\alpha)$ and g_{MN} is the D8-brane metric given in eq. (2.10). The first term in the action (3.1) arises from the α' expansion of the non-abelian Dirac Born Infeld action (see for instance [14]). The second term is the Chern-Simons action which is not relevant for the present discussion. We will set $A_\alpha = 0$ and assume that the other gauge field components do not depend on the S^4 coordinates. Then, we obtain a five dimensional effective action for gauge field fluctuations

$$S_{eff} = \kappa \int d^4x \int d\tilde{z} \text{tr} \left[\frac{1}{2} (K(\tilde{z}))^{-1/3} \eta^{\mu\lambda} \eta^{\nu\rho} F_{\lambda\rho} F_{\mu\nu} + M_{KK}^2 K(\tilde{z}) \eta^{\mu\nu} F_{\mu\tilde{z}} F_{\nu\tilde{z}} \right] \quad (3.2)$$

where we introduced the dimensionless variable $\tilde{z} = z/U_{KK}$ and

$$K(\tilde{z}) \equiv 1 + \tilde{z}^2, \quad \kappa = \frac{g_{YM}^2 N_c^2}{216\pi^3}. \quad (3.3)$$

In order to obtain a four dimensional effective action with external gauge fields we choose the gauge condition $A_{\tilde{z}} = 0$ and expand A_μ in the following way [2] :

$$A_\mu(x, \tilde{z}) = \hat{\mathcal{V}}_\mu(x) + \hat{\mathcal{A}}_\mu(x)\psi_0(\tilde{z}) + \sum_{n=1}^{\infty} v_\mu^n(x)\psi_{2n-1}(\tilde{z}) + \sum_{n=1}^{\infty} a_\mu^n(x)\psi_{2n}(\tilde{z}) \quad , \quad (3.4)$$

where $\psi_0(\tilde{z}) \equiv (2/\pi) \arctan \tilde{z}$ and

$$\begin{aligned} \hat{\mathcal{V}}_\mu(x) &= \frac{1}{2} e^{-\frac{i\Pi(x)}{f\pi}} [A_{L\mu}(x) + \partial_\mu] e^{\frac{i\Pi(x)}{f\pi}} + \frac{1}{2} e^{\frac{i\Pi(x)}{f\pi}} [A_{R\mu}(x) + \partial_\mu] e^{-\frac{i\Pi(x)}{f\pi}} \\ \hat{\mathcal{A}}_\mu(x) &= \frac{1}{2} e^{-\frac{i\Pi(x)}{f\pi}} [A_{L\mu}(x) + \partial_\mu] e^{\frac{i\Pi(x)}{f\pi}} - \frac{1}{2} e^{\frac{i\Pi(x)}{f\pi}} [A_{R\mu}(x) + \partial_\mu] e^{-\frac{i\Pi(x)}{f\pi}} . \end{aligned} \quad (3.5)$$

The field $\Pi(x)$ is interpreted as the pion field, the fields $A_{L\mu}(x)$ and $A_{R\mu}(x)$ represent external gauge fields while the fields $v_\mu^n(x)$ and $a_\mu^n(x)$ are related to vector and axial-vector mesons. Substituting (3.4) in (3.2) and imposing the conditions

$$\kappa \int d\tilde{z} (K(\tilde{z}))^{-1/3} \psi_r(\tilde{z}) \psi_s(\tilde{z}) = \delta_{rs} \quad , \quad (3.6)$$

$$-(K(\tilde{z}))^{1/3} \partial_{\tilde{z}} [K(\tilde{z}) \partial_{\tilde{z}} \psi_r(\tilde{z})] = \lambda_r \psi_r(\tilde{z}) \quad , \quad (3.7)$$

where r, s are positive integers, we obtain a 4d effective lagrangian where four dimensional vector and axial-vector mesons emerge as modes of the 5d flavor gauge fields after integrating out the \tilde{z} direction. The condition (3.6) is a usual orthonormality condition for the wave functions while the condition (3.7) consists on an infinite set of equations of motion for the $\psi_r(\tilde{z})$ modes.

The 4d effective lagrangian after convenient field redefinitions (and apart from divergent terms) is

$$\begin{aligned} \mathcal{L}_{eff}^{4d} &= \frac{1}{2} \text{tr} (\partial_\mu \tilde{v}_\nu^n - \partial_\nu \tilde{v}_\mu^n)^2 + \frac{1}{2} \text{tr} (\partial_\mu \tilde{a}_\nu^n - \partial_\nu \tilde{a}_\mu^n)^2 + \text{tr} (i\partial_\mu \Pi + f_\pi \mathcal{A}_\mu)^2 \\ &+ M_{v^n}^2 \text{tr} \left(\tilde{v}_\mu^n - \frac{g_{v^n}}{M_{v^n}^2} \mathcal{V}_\mu \right)^2 + M_{a^n}^2 \text{tr} \left(\tilde{a}_\mu^n - \frac{g_{a^n}}{M_{a^n}^2} \mathcal{A}_\mu \right)^2 + \sum_{j \geq 3} \mathcal{L}_j \end{aligned} \quad (3.8)$$

where \mathcal{L}_j represent the interaction terms of order j in the fields. The field redefinitions and constants are

$$\tilde{v}_\mu^n = v_\mu^n + \frac{g_{v^n}}{M_{v^n}^2} \mathcal{V}_\mu \quad , \quad \tilde{a}_\mu^n = a_\mu^n + \frac{g_{a^n}}{M_{a^n}^2} \mathcal{A}_\mu \quad , \quad (3.9)$$

$$\mathcal{V}_\mu = \frac{1}{2} (A_{L\mu} + A_{R\mu}) \quad , \quad \mathcal{A}_\mu = \frac{1}{2} (A_{L\mu} - A_{R\mu}) \quad (3.10)$$

$$M_{v^n}^2 = \lambda_{2n-1} M_{KK}^2 \quad , \quad M_{a^n}^2 = \lambda_{2n} M_{KK}^2 \quad , \quad (3.11)$$

$$g_{v^n} = \kappa M_{v^n}^2 \int d\tilde{z} K(\tilde{z})^{-1/3} \psi_{2n-1}(\tilde{z}) \quad , \quad (3.12)$$

$$g_{a^n} = \kappa M_{a^n}^2 \int d\tilde{z} K(\tilde{z})^{-1/3} \psi_{2n}(\tilde{z}) \psi_0(\tilde{z}) \quad , \quad (3.13)$$

The effective lagrangian (3.8) contains massive vector mesons \tilde{v}_μ^n , \tilde{a}_μ^n and a massless pion field Π . The constant g_{v^n} is the coupling between a vector meson \tilde{v}_μ^n and an external

$U(1)$ field \mathcal{V}_μ representing the photon. This is the only interaction between photons and mesons in the D4-D8 model. This is how vector meson dominance is realized in this model. The other constant g_{a^n} is the coupling between an axial-vector meson \tilde{a}_μ^n and an external axial $U(1)$ field \mathcal{A}_μ . This interaction does not contribute to electromagnetic form factors.

The part of the 4d interaction lagrangian \mathcal{L}_j that describes the cubic interaction among vector and axial-vector mesons is

$$\begin{aligned} \mathcal{L}_{int}^{4d} = & \text{tr} \left\{ (\partial^\mu \tilde{v}^{\nu n} - \partial^\nu \tilde{v}^{\mu n}) \left(g_{v^n v^\ell v^m} [\tilde{v}_\mu^\ell, \tilde{v}_\nu^m] + g_{v^n a^\ell a^m} [\tilde{a}_\mu^\ell, \tilde{a}_\nu^m] \right) \right. \\ & \left. + g_{v^\ell a^m a^n} (\partial^\mu \tilde{a}^{\nu n} - \partial^\nu \tilde{a}^{\mu n}) \left([\tilde{v}_\mu^\ell, \tilde{a}_\nu^m] - [\tilde{v}_\nu^\ell, \tilde{a}_\mu^m] \right) \right\}, \end{aligned} \quad (3.14)$$

where the three-meson coupling constants are given by

$$g_{v^n v^\ell v^m} = \kappa \int d\tilde{z} K(\tilde{z})^{-1/3} \psi_{2n-1}(\tilde{z}) \psi_{2\ell-1}(\tilde{z}) \psi_{2m-1}(\tilde{z}), \quad (3.15)$$

$$g_{v^\ell a^m a^n} = \kappa \int d\tilde{z} K(\tilde{z})^{-1/3} \psi_{2\ell-1}(\tilde{z}) \psi_{2m}(\tilde{z}) \psi_{2n}(\tilde{z}). \quad (3.16)$$

In order to obtain the masses M_{v^n} , M_{a^n} and the coupling constants g_{v^n} , $g_{v^n v^\ell v^m}$ and $g_{v^\ell a^m a^n}$ we will now calculate numerically the wave functions $\psi_r(\tilde{z})$.

3.1 Wave functions and Regge trajectories

Now we solve numerically the equations of motion for the vector and axial-vector modes using the *shooting method*, as done previously in [1]. First, we analyze the large \tilde{z} behavior of the $\psi_r(\tilde{z})$ functions. From the normalization condition (3.6) and equation of motion (3.7) we conclude that the ψ_r functions decrease asymptotically as \tilde{z}^{-1} when $\tilde{z} \rightarrow \pm\infty$. Then, it is convenient to define $\tilde{\psi}_r \equiv \tilde{z}\psi_r$. In terms of this function the equation of motion takes the form

$$\tilde{z}\partial_{\tilde{z}} \left[\tilde{z}\partial_{\tilde{z}} \tilde{\psi}_r \right] + A(\tilde{z}) \tilde{z}\partial_{\tilde{z}} \tilde{\psi}_r + B(\tilde{z}) \tilde{\psi}_r = 0, \quad (3.17)$$

where

$$\begin{aligned} A(\tilde{z}) &= -\frac{1+3\tilde{z}^{-2}}{1+\tilde{z}^{-2}} \equiv \sum_{\ell=0}^{\infty} A_\ell \tilde{z}^{-2\ell/3}, \\ B(\tilde{z}) &= 2\frac{\tilde{z}^{-2}}{1+\tilde{z}^{-2}} + \lambda_r \tilde{z}^{-2/3} (1+\tilde{z}^{-2})^{-4/3} \equiv \sum_{\ell=0}^{\infty} B_\ell \tilde{z}^{-2\ell/3}. \end{aligned} \quad (3.18)$$

The expansions defined in (3.18) are well behaved for large \tilde{z} . They suggest the following ansatz for $\tilde{\psi}_r$:

$$\tilde{\psi}_r(\tilde{z}) = \sum_{\ell=0}^{\infty} \alpha_\ell \tilde{z}^{-2\ell/3}, \quad (3.19)$$

with $\alpha_0 = 1$. Substituting (3.19) in (3.17) leads to the recurrence relations

$$\begin{aligned} \alpha_1 &= -\frac{9}{10} B_1, \\ \alpha_\ell &= \left(\frac{4}{9}\ell^2 + \frac{2}{3}\ell \right)^{-1} \left(\frac{2}{3} \sum_{k=1}^{\ell-1} k \alpha_k A_{\ell-k} - \sum_{k=0}^{\ell-1} \alpha_k B_{\ell-k} \right) \end{aligned} \quad (3.20)$$

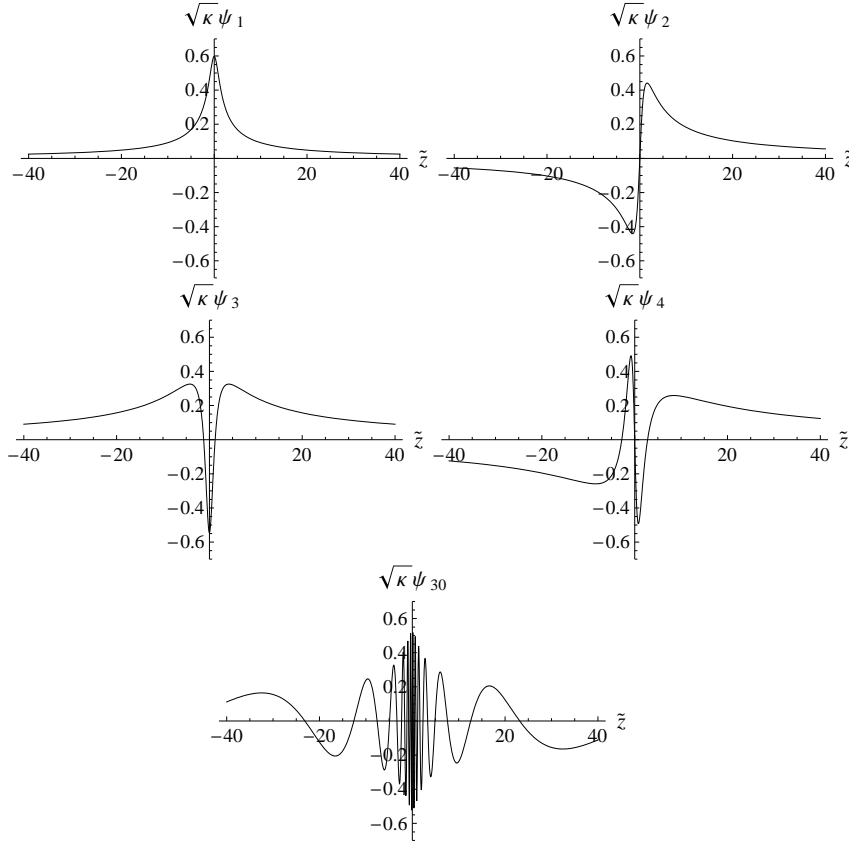


Figure 1: Wave functions $\psi_r(\tilde{z})$ multiplied by $\sqrt{\kappa}$ for the cases $r = 1, 2, 3, 4$ and $r = 30$.

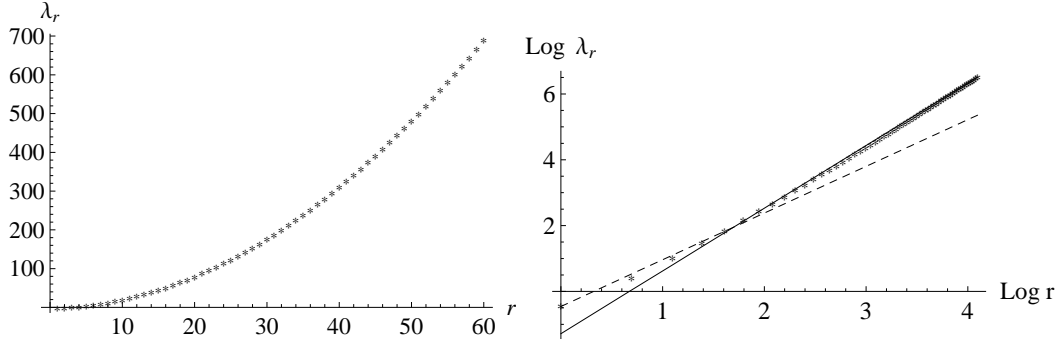


Figure 2: Vector and axial-vector meson Regge trajectory for D4-D8 model. The left panel shows the dependence of λ_r with the radial number $r = 1, 2, 3, \dots, 60$. In the right panel we plot a logarithmic graph of λ_r and two linear fits in different ranges: the dashed line corresponds to $-0.46 + 1.42 \log r$ for $r = \{1, 5\}$, while the solid line is $-1.28 + 1.91 \log r$ for $r = \{6, 60\}$.

Now we analyze the parity of the wave functions. The vector and axial-vector mesons transforms under parity in the following way

$$v_\mu^n(t, -\bar{x}) = v_\mu^n(t, \bar{x}) \quad , \quad a_\mu^n(t, -\bar{x}) = -a_\mu^n(t, \bar{x}) . \quad (3.21)$$

Such transformation exchange the gauge field chiral components, A_L and A_R . In order

to guarantee a five dimensional gauge field invariance under the parity transformation $(t, \bar{x}, \tilde{z}) \rightarrow (t, -\bar{x}, -\tilde{z})$ we impose the conditions

$$\psi_{2n}(-\tilde{z}) = \psi_{2n}(\tilde{z}) \quad , \quad \psi_{2n-1}(-\tilde{z}) = -\psi_{2n-1}(\tilde{z}) \quad (3.22)$$

If the $\psi_{2n}(\tilde{z})$ and $\psi_{2n-1}(\tilde{z})$ wave functions are regular at the origin $\tilde{z} = 0$ eq. (3.22) leads to the conditions

$$\partial_{\tilde{z}}\psi_{2n}(0) = 0 \quad , \quad \psi_{2n-1}(0) = 0. \quad (3.23)$$

Using these conditions at $\tilde{z} = 0$ and the large \tilde{z} behavior given by eq. (3.19), we solved numerically eq. (3.7), finding the solutions $\psi_r(z)$ and their eigenvalues λ_r for $r = 1$ to 60. We plot some wavefunctions in Figure 1. Note that the eigenfunctions $\psi_r(z)$ have an oscillatory behavior and the number of oscillations increases with λ_r . Looking at the small z limit of equation (3.7) one sees that it reduces to a sinusoidal wave equation with solutions:

$$\psi_{2n} \sim \sin(\sqrt{\lambda_{2n}} z), \quad \psi_{2n-1} \sim \cos(\sqrt{\lambda_{2n-1}} z). \quad (3.24)$$

So, one expects an oscillatory behavior in this region. For large z we observe the expected z^{-1} behavior.

The eigenvalues λ_r give us the vector and axial-vector quadratic masses $M_r^2 = \lambda_r M_{KK}^2$, according to equation (3.11). Notice that even values of r correspond to axial-vector mesons and odd values of r to vector mesons. In Figure 2 we show the dependence of λ_r on the radial number $r = 1, 2, 3, \dots, 60$. From the plots in this figure we conclude that vector and axial-vector mesons have the same radial Regge trajectory.

In the right panel of Figure 2 we plot a logarithmic graph and present two linear fits for different ranges of r . For $r = 1, \dots, 5$ the best linear fit is given by $-0.46 + 1.42 \log r$, so that in this region $\lambda_r \sim r^{1.42}$. For the region $r = \{6, 60\}$ the best fit is $-1.28 + 1.91 \log r$ corresponding to $\lambda_r \sim r^{1.91}$. Fitting the data for larger values of r , we conclude that the Regge trajectory for vector and axial-vector mesons in the D4-D8 model approaches an asymptotic quadratic behaviour $\lambda_r \sim r^2$. Such behaviour is similar to the ones found in hard-wall model [15–19] and the D3-D7 brane model [20, 21].

3.2 Coupling and decay constants

In order to calculate the elastic form factors for the lowest energy vector and axial-vector meson states, we must compute the vector meson decay constants g_{v^n} and the coupling constants between the intermediate vector meson and the external vector mesons $g_{v^n v^\ell v^m}$ and axial-vector mesons $g_{v^n a^\ell a^m}$. We calculated these coupling constants using eqs. (3.12), (3.15), (3.16) and our numerical results for the normalized wave functions ψ_{2n} and ψ_{2n-1} and the corresponding eigenvalues, for $n = 1, 2, \dots, 30$.

We show some numerical results for vector mesons in Table 1 and for axial-vector mesons in Table 2. Note that the decay constants are positive, increase monotonically with n and their ratio with the squared masses $g_{v^n}/M_{v^n}^2$ is approximately equal to $3.14\sqrt{\kappa}$. On the other hand, the vector meson couplings $g_{v^n v^\ell v^m}$ and $g_{v^n a^\ell a^m}$ do not present a simple dependence with n but oscillate (irregularly) with it. Nonetheless, these coupling constants obey sum rules that are crucial for the hadronic form factors, as we will discuss in the following section.

n	$\frac{M_{n,n}^2}{M_{KK}^2}$	$\frac{g_{v,n}}{\sqrt{\kappa}M_{KK}^2}$	$\sqrt{\kappa}g_{v^n v^1 v^1}$	$\sqrt{\kappa}g_{v^n v^2 v^2}$	$\sqrt{\kappa}g_{v^n v^1 v^2}$
1	0.6693	2.109	0.4466	0.2687	-0.1465
2	2.874	9.108	-0.1465	0.04261	0.2687
3	6.591	20.80	0.01843	0.1209	-0.1477
4	11.80	37.15	-3.689×10^{-4}	-0.1483	0.02371
5	18.49	58.17	2.695×10^{-4}	0.03169	-1.921×10^{-4}
6	26.67	83.83	3.078×10^{-5}	3.000×10^{-4}	4.469×10^{-4}
7	36.34	114.2	1.857×10^{-5}	7.924×10^{-4}	7.560×10^{-5}
8	47.49	149.1	6.996×10^{-6}	1.824×10^{-4}	4.080×10^{-5}
9	60.14	188.7	3.508×10^{-6}	9.417×10^{-5}	1.723×10^{-5}

Table 1: Dimensionless squared masses and coupling constants for vector mesons.

n	$\frac{M_{a,n}^2}{M_{KK}^2}$	$\sqrt{\kappa}g_{v^n a^1 a^1}$	$\sqrt{\kappa}g_{v^n a^2 a^2}$	$\sqrt{\kappa}g_{v^n a^1 a^2}$
1	1.569	0.2865	0.2572	-0.1453
2	4.546	0.1475	0.03770	0.1345
3	9.008	-0.1438	0.03294	0.1248
4	14.96	0.02617	0.1007	-0.1465
5	22.39	8.738×10^{-5}	-0.1491	0.03023
6	31.32	5.312×10^{-4}	0.03552	1.995×10^{-4}
7	41.73	9.789×10^{-5}	6.837×10^{-4}	7.289×10^{-4}
8	53.63	5.144×10^{-5}	1.033×10^{-3}	1.622×10^{-4}
9	67.02	2.212×10^{-5}	2.721×10^{-4}	8.421×10^{-5}

Table 2: Dimensionless squared masses and coupling constants for axial-vector mesons.

4. Form Factors

The electromagnetic form factor represents the interaction of a particle with an external photon. Here we will calculate these form factors for vector and axial-vector mesons. As shown in [2], photon-meson-meson couplings are all cancelled in the D4-D8 model. This means that the photon interacts with a meson only through intermediate vector mesons. This is a realization of vector meson dominance (VMD) in electromagnetic scattering in this model.

In order to calculate the form factors we first obtain a general expression valid for the elastic and non-elastic cases. Then, for the elastic case, we calculate the electric, magnetic, quadrupole form factors as well as the longitudinal, transverse and longitudinal-transverse

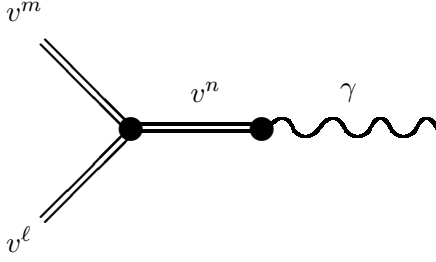


Figure 3: Feynman diagram for vector meson form factor. A similar diagram holds for the axial-vector meson replacing the external lines v^m, v^ℓ by a^m, a^ℓ .

form factors. Also, for the first vector and axial-vector excitations, $\rho(770)$ and $a_1(1260)$, we calculate the electric radius and the magnetic and quadrupole moments. We end this section with a brief discussion of the so called transition (non-elastic) form factors.

The form factors are calculated from the matrix elements of the electromagnetic current. The interaction of a vector meson with an off-shell photon is described by the matrix element

$$\langle v^{m a}(p), \epsilon | \tilde{J}^{\mu c}(q) | v^{\ell b}(p'), \epsilon' \rangle = (2\pi)^4 \delta^4(p' - p - q) \langle v^{m a}(p), \epsilon | J^{\mu c}(0) | v^{\ell b}(p'), \epsilon' \rangle, \quad (4.1)$$

where v^m and v^ℓ are the initial and final vector meson states with momenta p and $p' = p + q$ and polarizations ϵ and ϵ' . The operator \tilde{J}^μ is the Fourier transform of the electromagnetic current $J^\mu(x)$. This matrix element is calculated from the corresponding Feynman diagram shown in Figure 3. From the effective lagrangian (3.8), together with the interaction terms (3.14), we find

$$\begin{aligned} \langle v^{m a}(p), \epsilon | J^{\mu c}(0) | v^{\ell b}(p'), \epsilon' \rangle &= \epsilon^\nu \epsilon'^\rho f^{abc} [\eta_{\sigma\nu}(q-p)_\rho + \eta_{\nu\rho}(2p+q)_\sigma - \eta_{\rho\sigma}(p+2q)_\nu] \\ &\times \sum_{n=1}^{\infty} g_{v^n} g_{v^m v^n v^\ell} \left[\frac{\eta^{\mu\sigma} + \frac{q^\mu q^\sigma}{M_{v^n}^2}}{q^2 + M_{v^n}^2} \right] \end{aligned} \quad (4.2)$$

where f^{abc} is the structure constant of $U(N_f)$ and M_{v^n} is the mass of the vector meson v^n . Using the sum rule

$$\sum_{n=1}^{\infty} \frac{g_{v^n} g_{v^n v^m v^\ell}}{M_{v^n}^2} = \delta_{m\ell} \quad (4.3)$$

obtained in [2], we find

$$\begin{aligned} \langle v^{m a}(p), \epsilon | J^{\mu c}(0) | v^{\ell b}(p'), \epsilon' \rangle &= \epsilon^\nu \epsilon'^\rho f^{abc} [\eta_{\sigma\nu}(q-p)_\rho + \eta_{\nu\rho}(2p+q)_\sigma - \eta_{\rho\sigma}(p+2q)_\nu] \\ &\times \left\{ \left(\eta^{\mu\sigma} - \frac{q^\mu q^\sigma}{q^2} \right) F_{v^m v^\ell}(q^2) + \delta_{m\ell} \frac{q^\mu q^\sigma}{q^2} \right\} \end{aligned} \quad (4.4)$$

where the generalized vector meson form factor is defined by

$$F_{v^m v^\ell}(q^2) = \sum_{n=1}^{\infty} \frac{g_{v^n} g_{v^n v^m v^\ell}}{q^2 + M_{v^n}^2}. \quad (4.5)$$

Taking into account the transversality of the vector meson polarizations: $\epsilon \cdot p = 0 = \epsilon' \cdot p'$, we obtain

$$\begin{aligned} & \langle v^{m a}(p), \epsilon | J^{\mu c}(0) | v^{\ell b}(p'), \epsilon' \rangle \\ &= \epsilon^\nu \epsilon'^\rho f^{abc} [\eta_{\nu\rho}(2p+q)_\sigma + 2(\eta_{\sigma\nu}q_\rho - \eta_{\rho\sigma}q_\nu)] \left(\eta^{\mu\sigma} - \frac{q^\mu q^\sigma}{q^2} \right) F_{v^m v^\ell}(q^2). \end{aligned} \quad (4.6)$$

Note that the term involving the factor $\delta_{m\ell}$ in eq. (4.4) did not contribute since in the elastic case ($m = \ell$) we have: $2p \cdot q + q^2 = 0$. Note also that this matrix element satisfies the transversality condition $q_\mu \langle v^m | J^\mu(0) | v^\ell \rangle = 0$.

In a similar way, for axial-vector mesons we can calculate the form factors from the matrix element $\langle a^{m a}(p), \epsilon | J^{\mu c}(0) | a^{\ell b}(p'), \epsilon' \rangle$. This corresponds to evaluating Feynman diagrams similar to Fig. 3, but with the external vector meson lines replaced by the axial-vector mesons a^m and a^ℓ . Note that the internal vector meson line v^n , representing vector meson dominance, is unchanged. Thus, the generalized axial-vector meson form factor is

$$F_{a^m a^\ell}(q^2) = \sum_{n=1}^{\infty} \frac{g_{v^n} g_{v^n a^m a^\ell}}{q^2 + M_{v^n}^2}. \quad (4.7)$$

4.1 Elastic case

The elastic form factor for vector mesons can be obtained considering the previous calculation with the same vector meson v^m in the initial and final states. Then, from eq. (4.6) we find

$$\begin{aligned} & \langle v^{m a}(p), \epsilon | J^{\mu c}(0) | v^{m b}(p'), \epsilon' \rangle \\ &= f^{abc} \{ (\epsilon \cdot \epsilon')(2p+q)^\mu + 2 [\epsilon^\mu (\epsilon' \cdot q) - \epsilon'^\mu (\epsilon \cdot q)] \} F_{v^m}(q^2), \end{aligned} \quad (4.8)$$

where $F_{v^m}(q^2)$ is the elastic form factor:

$$F_{v^m}(q^2) = \sum_{n=1}^{\infty} \frac{g_{v^n} g_{v^n v^m v^m}}{q^2 + M_{v^n}^2}. \quad (4.9)$$

Note that eqs. (4.8) and (4.9) are also valid for the axial-vector mesons, replacing v^m by a^m . We calculated numerically these sums from $n = 1$ to $n = 30$ using the results obtained for the masses and couplings. We adopted $M_{\kappa\kappa} = 0.946$ GeV, as in ref. [1]. We plot in Figure 4 the elastic form factors for the vector meson $\rho(770)$ (v^1) and axial-vector meson $a_1(1260)$ (a^1). Note that when $q^2 \rightarrow 0$, the vector and axial-vector form factors go to one, thanks to the sum rule (4.3).

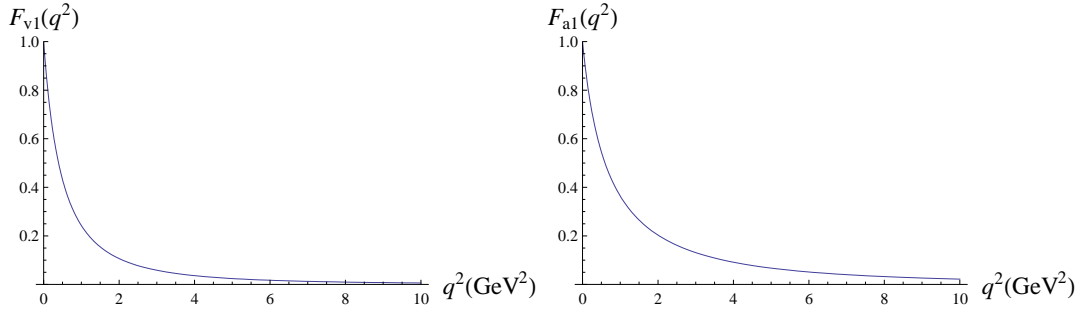


Figure 4: Elastic form factors for v^1 and a^1 .

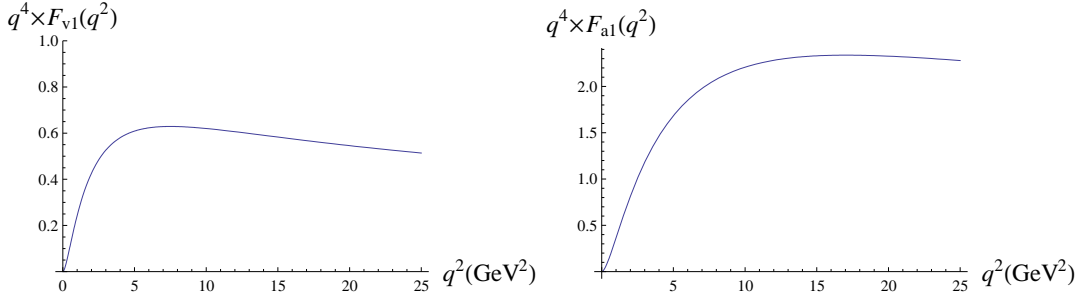


Figure 5: q^4 times the elastic form factors for v^1 and a^1 .

Let us now investigate the large q^2 behaviour of the elastic factors. Performing an expansion in powers of q^{-2} :

$$\begin{aligned}
 F_{v^m}(q^2) &= \frac{1}{q^2} \sum_{n=1}^{\infty} g_{v^n} g_{v^n v^m v^m} \left(1 - \frac{M_{v^n}^2}{q^2} + \mathcal{O}(q^{-4}) \right) \\
 F_{a^m}(q^2) &= \frac{1}{q^2} \sum_{n=1}^{\infty} g_{v^n} g_{v^n a^m a^m} \left(1 - \frac{M_{v^n}^2}{q^2} + \mathcal{O}(q^{-4}) \right), \quad (4.10)
 \end{aligned}$$

we see that the dominant terms would be of order q^{-2} . We calculated the coefficients of these terms using our numerical results with $n = 1, \dots, 30$. We found

$$\begin{aligned}
 \sum_{n=1}^{30} g_{v^n} g_{v^n v^1 v^1} &\approx 0.0005835(\text{GeV})^2, & \sum_{n=1}^{30} g_{v^n} g_{v^n a^1 a^1} &\approx 0.0001485(\text{GeV})^2, \\
 \sum_{n=1}^{30} g_{v^n} g_{v^n v^2 v^2} &\approx -0.0002939(\text{GeV})^2, & \sum_{n=1}^{30} g_{v^n} g_{v^n a^2 a^2} &\approx -0.002043(\text{GeV})^2 \\
 \sum_{n=1}^{30} g_{v^n} g_{v^n v^3 v^3} &\approx -0.003339(\text{GeV})^2, & \sum_{n=1}^{30} g_{v^n} g_{v^n a^3 a^3} &\approx -0.007522(\text{GeV})^2. \quad (4.11)
 \end{aligned}$$

These results indicate that the following superconvergence relations hold in the D4-D8 model:

$$\sum_{n=1}^{\infty} g_{v^n} g_{v^n v^m v^m} = 0, \quad \sum_{n=1}^{\infty} g_{v^n} g_{v^n a^m a^m} = 0, \quad (4.12)$$

so, from eqs. (4.10) we expect that the form factors decrease approximately as q^{-4} , for large q^2 .

In order to investigate this behaviour, we plot in Figure 5 the form factors for the first vector and axial-vector states multiplied by q^4 . We also plotted the elastic form factors for the first three excited states multiplied by q^4 in Figure 6.

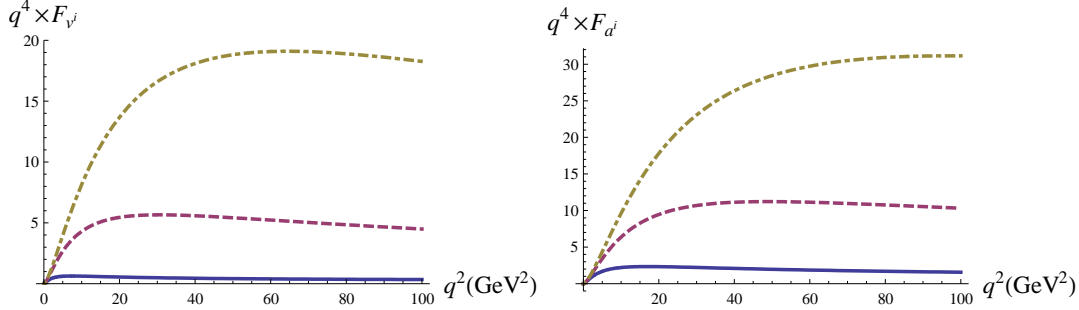


Figure 6: q^4 times the elastic form factors for vector and axial-vector mesons for the first three states: $i = 1$ (solid line), 2 (dashed line), 3 (dot-dashed line). Left panel: F_{v_i} . Right panel: F_{a_i} .

We conclude that the form factors approximately decrease as q^{-4} , for large q^2 , within the numerical errors. The deviation from the q^{-4} dependence is associated with the non-vanishing of the numerical sums (4.11).

Electric, magnetic and quadrupole form factors

The matrix element of the electromagnetic current for a spin one particle in the elastic case can be decomposed as [8]

$$\begin{aligned} \langle p, \epsilon | J_{EM}^\mu(0) | p', \epsilon' \rangle &= (\epsilon \cdot \epsilon') (2p + q)^\mu F_1(q^2) + [\epsilon^\mu (\epsilon' \cdot q) - \epsilon'^\mu (\epsilon \cdot q)] [F_1(q^2) + F_2(q^2)] \\ &+ \frac{1}{p^2} (q \cdot \epsilon') (q \cdot \epsilon) (2p + q)^\mu F_3(q^2). \end{aligned} \quad (4.13)$$

From F_1, F_2 and F_3 we can define

$$F_E = F_1 + \frac{q^2}{6p^2} \left[F_2 - \left(1 - \frac{q^2}{4p^2}\right) F_3 \right], \quad F_M = F_1 + F_2, \quad F_Q = -F_2 + \left(1 - \frac{q^2}{4p^2}\right) F_3 \quad (4.14)$$

where F_E, F_M and F_Q are the electric, magnetic, and quadrupole form factors. From eqs. (4.8) and (4.13) we find that for a vector meson v^m

$$F_1^{(v^m)} = F_2^{(v^m)} = F_{v^m}, \quad F_3^{(v^m)} = 0, \quad (4.15)$$

where F_{v^m} is given by eq. (4.9). Hence the electric, magnetic and quadrupole form factors predicted by the D4-D8 brane model for vector mesons are

$$F_E^{(v^m)} = \left(1 + \frac{q^2}{6p^2}\right) F_{v^m}, \quad F_M^{(v^m)} = 2F_{v^m}, \quad F_Q^{(v^m)} = -F_{v^m}. \quad (4.16)$$

The same results hold for the axial-vector mesons a^m . From these form factors we can estimate three important physical quantities associated with the vector mesons: the electric radius, the magnetic and quadrupole moments.

The electric radius for the vector and axial-vector mesons are given by

$$\langle r_{v^m}^2 \rangle = -6 \frac{d}{dq^2} F_E^{(v^m)}(q^2)|_{q^2=0} , \quad \langle r_{a^m}^2 \rangle = -6 \frac{d}{dq^2} F_E^{(a^m)}(q^2)|_{q^2=0} . \quad (4.17)$$

Using our numerical results for the form factors for the lowest excited states ρ and a_1 , we find the electric radii:

$$\langle r_\rho^2 \rangle = 0.5739 \text{ fm}^2 , \quad \langle r_{a_1}^2 \rangle = 0.4061 \text{ fm}^2 . \quad (4.18)$$

The magnetic and quadrupole moments are defined by

$$\mu \equiv F_M(q^2)|_{q^2=0} , \quad D \equiv -\frac{1}{p^2} F_Q(q^2)|_{q^2=0} . \quad (4.19)$$

Using the fact that F_{v^m} and F_{a^m} go to one when $q^2 \rightarrow 0$, we obtain

$$\mu_{v^m} = \mu_{a^m} = 2 , \quad D_{v^m} = -\frac{1}{M_{v^m}^2} , \quad D_{a^m} = -\frac{1}{M_{a^m}^2} . \quad (4.20)$$

Our results for electric radius, magnetic and quadrupole moments for the vector meson ρ are in agreement with the hard wall model results found in [8].

Decomposition in terms of transverse and longitudinal polarizations

It is interesting to calculate also the form factors of vector mesons with specific polarizations [22]. A vector particle with mass M and four momentum $(E, 0, 0, p_z)$ has three independent polarizations that can be written as

$$\epsilon_T^1 = (0, 1, 0, 0) , \quad \epsilon_T^2 = (0, 0, 1, 0) , \quad \epsilon_L = (p_z/M, 0, 0, E/M) . \quad (4.21)$$

When studying the elastic scattering of a photon and a vector meson in the Breit frame, the initial and final four momenta of the vector meson take, respectively, the forms $p = (E, 0, 0, -q/2)$, and $p' = (E, 0, 0, q/2)$. In this frame we define the form factors

$$\begin{aligned} F_{TT}(q^2) &= \frac{\langle p, \epsilon_T | J_0(0) | p', \epsilon'_T \rangle}{2E} , & F_{LT}(q^2) &= \frac{\langle p, \epsilon_T | J_x(0) | p', \epsilon'_L \rangle}{2E} \\ F_{LL}(q^2) &= \frac{\langle p, \epsilon_L | J_0(0) | p', \epsilon'_L \rangle}{2E} . \end{aligned} \quad (4.22)$$

From eq. (4.8) we find

$$F_{TT}^{(v^m)} = F_{v^m} , \quad F_{LT}^{(v^m)} = \frac{q}{M_{v^m}} F_{v^m} , \quad F_{LL}^{(v^m)} = \left(1 - \frac{q^2}{2M_{v^m}^2} \right) F_{v^m} . \quad (4.23)$$

The large q^2 behavior of these form factors in the D4-D8 model is determined from F_{v^m} , eq. (4.9). We obtain the asymptotic behaviors: $F_{TT}^{(v^m)} \sim q^{-4}$, $F_{LT}^{(v^m)} \sim q^{-3}$, $F_{LL}^{(v^m)} \sim q^{-2}$, in agreement with QCD calculations (see for instance [22]).

4.2 Non-elastic case

When the initial and final meson states are different, the interaction with the photon is described by the generalized form factors of eqs. (4.5), (4.7), when $m \neq \ell$, also known as transition form factors. We calculated these form factors for an initial vector meson in the lowest state v^1 and final states v^2, v^3, v^4 . We also calculated the transitions form factors for the initial axial-vector meson a^1 and final a^2, a^3, a^4 .

We illustrate in Figure 7 the dependence of these form factors with the momentum transfer q^2 , compared with the corresponding elastic form factors. We see that the transition form factors vanish as $q^2 \rightarrow 0$, in contrast to the elastic form factors that approach the unit in this limit. Note that as q^2 increases from zero, first F_{v^1} dominates, then $F_{v^1 v^2}$ dominates, then $F_{v^1 v^3}$, and so on. The same situation occurs for the axial-vector case. Physically, this corresponds to the fact that as the momentum transfer increases, the amplitude for producing heavier final states increases as well.

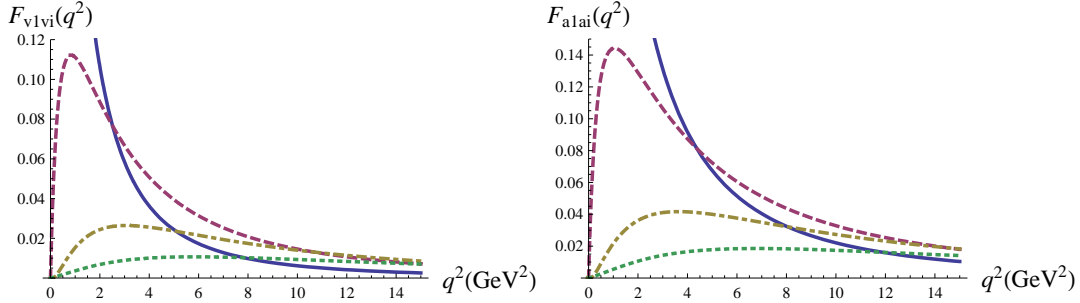


Figure 7: Transition form factors. Left panel: $F_{v^1 v^i}$, right panel: $F_{a^1 a^i}$, for $i = 1$ (solid line), 2 (dashed line), 3 (dot-dashed line), 4 (dotted line). The solid lines corresponding to $i = 1$ approaches one as $q^2 \rightarrow 0$.

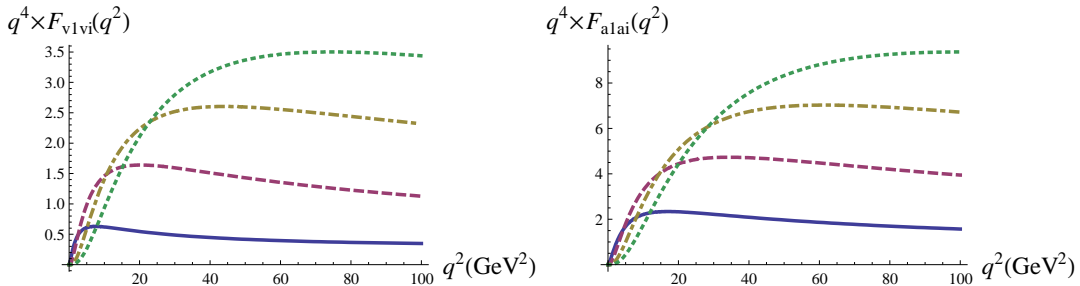


Figure 8: q^4 times the form factors. Left panel: $F_{v^1 v^i}$, right panel: $F_{a^1 a^i}$, for $i = 1$ (solid line), 2 (dashed line), 3 (dot-dashed line), 4 (dotted line).

Regarding the large q^2 dependence of these non-elastic form factors, we can make an expansion similar to eq. (4.10) but for different initial and final states. If the following superconvergence relations hold:

$$\sum_{n=1}^{\infty} g_{v^n} g_{v^n v^m v^l} = 0, \quad \sum_{n=1}^{\infty} g_{v^n} g_{v^n a^m a^l} = 0. \quad (4.24)$$

we should find a q^{-4} behavior as we found in the elastic case. We calculated these sums from $n = 1, \dots, 30$, for the relevant states, finding:

$$\begin{aligned}
\sum_{n=1}^{30} g_{v^n} g_{v^n v^1 v^2} &\approx -0.000367(\text{GeV})^2, & \sum_{n=1}^{30} g_{v^n} g_{v^n a^1 a^2} &\approx -0.0007793(\text{GeV})^2, \\
\sum_{n=1}^{30} g_{v^n} g_{v^n v^1 v^3} &\approx -0.0002850(\text{GeV})^2, & \sum_{n=1}^{30} g_{v^n} g_{v^n a^1 a^3} &\approx -0.001863(\text{GeV})^2, \\
\sum_{n=1}^{30} g_{v^n} g_{v^n v^1 v^4} &\approx -0.001190(\text{GeV})^2, & \sum_{n=1}^{30} g_{v^n} g_{v^n a^1 a^4} &\approx -0.001484(\text{GeV})^2. \quad (4.25)
\end{aligned}$$

These results indicate the validity of relations (4.24).

In order to check the large q^2 behavior, we plot in Figure 8 the transition form factors multiplied by q^4 , and the corresponding elastic form factors for comparison. We conclude that the transition form factors approach asymptotically the expected q^{-4} dependence.

5. Conclusion

In this work we investigated the electromagnetic scattering of vector and axial-vector mesons in the D4-D8 model. We calculated the elastic and transition meson form factors and found the expected behaviour at small and large momentum transfer q^2 . In the elastic case, we calculated the magnetic and quadrupole moments and, for the mesons ρ and a_1 , the electric radii. We also analyzed the momentum dependence of F_{TT} , F_{LT} and F_{LL} at large q^2 finding a QCD like asymptotic behaviour.

Our analysis of the form factor momentum dependence led us to non-trivial sum rules for the vector and axial-vector coupling constants. These sum rules generalize the superconvergence rule previously obtained within the hard wall model for the elastic case [8].

Although the D4-D8 brane model was originally proposed to describe the low energy regime of QCD, our results suggest that vector meson form factors at intermediate and high energies show a q^2 dependence consistent with QCD expectations. It would be interesting to investigate if other aspects of hadronic scattering at high energy could be described by this holographic model.

Acknowledgments: The authors are partially supported by Capes, CNPq and FAPERJ.

References

- [1] T. Sakai and S. Sugimoto, Prog. Theor. Phys. **113** (2005) 843 [arXiv:hep-th/0412141].
- [2] T. Sakai and S. Sugimoto, Prog. Theor. Phys. **114** (2005) 1083 [arXiv:hep-th/0507073].
- [3] H. Hata, T. Sakai, S. Sugimoto and S. Yamato, [arXiv:hep-th/0701280].
- [4] K. Hashimoto, T. Sakai and S. Sugimoto, Prog. Theor. Phys. **120** (2008) 1093 [arXiv:0806.3122 [hep-th]].
- [5] K. Hashimoto, T. Sakai and S. Sugimoto, [arXiv:0901.4449 [hep-th]].

- [6] M. Gell-Mann and F. Zachariasen, *Phys. Rev.* **124**, 953 (1961).
- [7] J. J. Sakurai, *Currents and Mesons*, Chicago Univ. Press, Chicago, 1969.
- [8] H. R. Grigoryan and A. V. Radyushkin, *Phys. Lett. B* **650**, 421 (2007) [arXiv:hep-ph/0703069].
- [9] S. Hong, S. Yoon and M. J. Strassler, *JHEP* **0404**, 046 (2004) [arXiv:hep-th/0312071].
- [10] S. Hong, S. Yoon and M. J. Strassler, *JHEP* **0604**, 003 (2006) [arXiv:hep-th/0409118].
- [11] H. R. Grigoryan and A. V. Radyushkin, *Phys. Rev. D* **76**, 095007 (2007) [arXiv:0706.1543 [hep-ph]].
- [12] S. J. Brodsky and G. F. de Teramond, *Phys. Rev. D* **77**, 056007 (2008) [arXiv:0707.3859 [hep-ph]].
- [13] J. Erdmenger, N. Evans, I. Kirsch and E. Threlfall, *Eur. Phys. J. A* **35**, 81 (2008) [arXiv:0711.4467 [hep-th]].
- [14] A. A. Tseytlin, *Nucl. Phys. B* **501**, 41 (1997) [arXiv:hep-th/9701125].
- [15] H. Boschi-Filho and N. R. F. Braga, *JHEP* **0305**, 009 (2003) [arXiv:hep-th/0212207].
- [16] H. Boschi-Filho and N. R. F. Braga, *Eur. Phys. J. C* **32**, 529 (2004) [arXiv:hep-th/0209080].
- [17] G. F. de Teramond and S. J. Brodsky, *Phys. Rev. Lett.* **94**, 201601 (2005) [arXiv:hep-th/0501022].
- [18] J. Erlich, E. Katz, D. T. Son and M. A. Stephanov, *Phys. Rev. Lett.* **95**, 261602 (2005) [arXiv:hep-ph/0501128].
- [19] H. Boschi-Filho, N. R. F. Braga and H. L. Carrion, *Phys. Rev. D* **73**, 047901 (2006) [arXiv:hep-th/0507063].
- [20] M. Kruczenski, D. Mateos, R. C. Myers and D. J. Winters, *JHEP* **0307**, 049 (2003) [arXiv:hep-th/0304032].
- [21] I. Kirsch, *JHEP* **0609**, 052 (2006) [arXiv:hep-th/0607205].
- [22] B. L. Ioffe and A. V. Smilga, *Nucl. Phys. B* **216**, 373 (1983).